

N78

19046

UNCLAS

DESIGN AND DEVELOPMENT OF A SOLAR ARRAY DRIVE

By Terence Rees and John M. Standing

Space Division
Hawker Siddeley Dynamics Limited,
Stevenage, Hertfordshire, England.

ABSTRACT

The design and development of a dry lubricated direct drive solar array pointing mechanism is discussed from its inception in 1970 to its present development into a flight mechanism for use on the Orbital Test Satellite (OTS), MAROTS, European Communication Satellite (ECS) and others. Results of life testing the original prototype and the OTS mechanism are presented together with an appraisal of expected future development.

INTRODUCTION

Since 1970, the European Space Agency has been concerned with developing the technology required for three-axis stabilised geostationary communications spacecraft. The Orbital Test Satellite (OTS) is scheduled for launch on a Thor-Delta in June, 1977, and associated contracts for the maritime version of OTS, MAROTS, and the European Communications Satellite (ECS) are in progress. In anticipation of these programmes, ESA placed a design and development contract for prototype Low Speed Mechanisms (LSM), the purpose being to establish the technology of slow speed despun mechanisms and solar array drives. At the start of this development precise requirements linked to a spacecraft application were not available, and in order to ensure that future applications would not cause fundamental changes in philosophy, severe design requirements were imposed. Within the LSM programme two mechanisms were manufactured and tested successfully providing the basis for the design of the Solar Array Drive for OTS. This OTS design is being applied, with little or no modification, to the Ariane Test Satellite, EXOSAT, MAROTS and ECS.

DESIGN OF THE LOW SPEED MECHANISM

Early in the LSM programme it became evident that the likely application was as a solar array drive. Consequently, emphasis was placed on a normal operational speed of 1 revolution/day and an acquisition, or slew speed of $10^\circ/\text{sec}$. The basic design requirements are given in Table 1.

The design of the LSM was conceived to be of modular form, that is, a self contained bearing and motor assembly with the slipring and brush blocks cantilevered from one end, allowing changes to the ring configuration as required. The overall assembly is shown in Figure 1. As can be seen, the drive is direct, with an Aeroflex brushless motor acting on the driven shaft. This approach was selected as it promised simplicity and low mass. Detailed analogue simulations were made to demonstrate the feasibility of the control concept.

The low speed and long life in a vacuum environment are requirements that can best be met by dry lubricants, as there is no advantage from an elastohydro-dynamically generated film normally associated with medium to high speed oil lubricated applications. During the design phase suitable lubricants were found; the ESA sponsored lead film for ball bearings, and a molybdenum disulphide/silver/copper composite brush material. Use of these lubricants avoids the need for reservoirs and molecular seals.

The specified temperature range and shaft to housing differential temperatures required careful selection of materials and the method of preloading the bearings. Duplex bearings provide good stiffness but are sensitive to temperature differentials in regard to preload and friction torque. The bearing arrangement selected has two angular contact bearings, one with inner and outer races clamped to the shaft and housing, the other being clamped to the shaft but having its outer race supported by a flexible diaphragm. This diaphragm takes up any axial differential expansions between the housing and shaft and is also used to apply a preload of 45N by means of a built-in deflection. Preload changes over the design temperature range are less than 10%.

The effect of having a hot shaft and colder housing is to reduce the internal clearances in the bearings with possible seizure of the mechanism. For the analysis it is assumed that the bearing races follow the radial expansions of the housing and shaft. Figures 2 and 3 show the effect of temperature differentials for combinations of beryllium for both the housing and shaft and aluminium for the housing and shaft. Beryllium is clearly superior. The bearing fits into the housing and allows a radial clearance of some 5 to 15 μm , the outer race being clamped by a plate. Friction between the race and the clamp plate will cause the bearing to distort by 1.5 to 5 μm radially before interfacial slip occurs. These distortions are detrimental to bearing torque. Similar remarks can be made about the fit to the shaft. Thermal modelling has shown that temperature differentials between the races and the corresponding mounting surfaces to be less than 10°C. Using beryllium to match the coefficient of expansion of the bearing steel therefore produces minimal bearing distortion. Titanium is competitive with beryllium but does not offer the mass advantages. The design finally selected employs beryllium for the housing and shaft with a titanium diaphragm integral with the carrier of the inboard bearing outer race. In the event this produced a bearing mounting and a preload loop which was highly insensitive to temperature.

Separable angular contact bearings are used so that the rotating assembly is stiff in one direction, and, due to the diaphragm, compliant in the other. To prevent the mechanism 'rattling' under the launch environment, and to avoid damage to the diaphragm the bearing system is caged. The off-loading mechanism comprises a conical face at the outboard bearing which meets a seat in the housing when in the launch configuration. To achieve this the shaft is displaced axially through 0.13mm by a pivoted lever which applies a preload to prevent separation of the conical faces. Release is obtained by pyrotechnic action.

Slipring design is conventional with an epoxy-moulding carried on a central aluminium tube. The contact surface at the slipring is electroplated silver and each ring has redundant brushes with separate running tracks. Both brushes are arranged to trail.

ESA were interested in correlating friction with angular position and required a shaft position readout to within 0.1° . This was accomplished over the full temperature range by use of a Gray code optical encoder giving 4096 counts per revolution. The encoder features a 15 track chrome on glass pattern illuminated by redundant light emitting diodes (LED) acting through a fibre optic bundle to provide a slit source. Operation of this encoder at the higher temperature proved troublesome due to the reduction in output from the LED's. However, improved heat sinking overcame this problem. Dissipation from the LED's forced the adoption of pulsed operation at 400Hz with a duty cycle of 5%, the position being sampled and stored between pulses. The encoder output is used to provide an error compared to a clock demanded position and also to commutate the Aeroflex brushless dc torque motor. Use of this encoder was limited to the research programme and development into a flight item was not foreseen, but the use of incremental encoders of the Moire fringe type promise low mass and high accuracy.

TEST HISTORY OF THE LSM

Prior to thermal vacuum testing correct operation was demonstrated for a range of solar paddle characteristics. The solar paddle simulators are suspended on a small bearing so that a weightless load is obtained with only a slight increase in friction. Flexibility is obtained by coupling the load to the mechanism by a torsion bar. The first simulator corresponded to a large solar array at 20kgm² inertia and 0.5Hz torsional frequency and was used to test the number one LSM. For the second LSM a simulator having a range of frequencies of 0.06 to 3.6Hz with an inertia of 2.8kgm² was used.

The first LSM was subjected to qualification levels of vibration and thermal vacuum testing prior to an accelerated life test equivalent to 10 years operation. A speed of 1 rev/hour was used, this being felt to be justified since the normal motion is stepped and a times 24 increase in speed merely increases the step frequency and does not change the motion within a step.

It was not possible to simulate the solar paddle inertia and flexibility in the test chamber but the sliprings did carry power. The life test cycle is shown in Table 2. Throughout testing the insensitivity of the mechanism to temperature was demonstrated. Figure 4 gives a typical trace obtained during the eclipse simulation, in which the drive flange temperature is reduced from 60 to -20°C in 72 minutes with the radiation 'sink' surrounding the mechanism held at 35°C . The variation in lag angle is ± 1 encoder division ($\pm 0.09^{\circ}$), that is approximately $\pm 0.0002\text{Nm}$ friction torque variation.

Strip down of the mechanism was carried out on completion of the 10 year equivalent life test. The condition of the mechanism was found to be excellent, with very little evidence of wear.

The second mechanism has completed over two years of testing at 1 revolution/day, the test cycle being as shown in Table 2 part B. Of some significance, is the data collected to date which shows a gradual reduction in friction. This is discussed below, together with similar findings from the OTS solar array drive. Table 3 summarises the real time test data.

SYSTEM PHILOSOPHY FOR A FLIGHT ARRAY DRIVE

Due to the criticality of the solar array drive system to mission success, particular attention had to be paid to reliability and the elimination of single point failures. Other areas of concern are minimising spacecraft body perturbations resulting from array motion, the impact of spacecraft contaminants on the performance of the array drive sliprings and the ability to control array sun pointing in the absence of the prime control signals.

A number of candidate solutions were investigated and included a stepper motor drive controlled by a spacecraft 'clock', a brushless or brushed d.c. motor controlled by a clock and a shaft position indicator, such as a resolver or optical encoder. The system finally chosen was to have a totally redundant sensing and drive system with the control signals being generated by solar array mounted sun sensors. A block diagram of a single channel is shown in Figure 5.

Each sensor provides two outputs, one being level detected within the electronics to indicate that the sun lies within the field of view of the sensor, the other giving a measure of the angle between the satellite sun vector and the normal to the array. In the normal sun tracking mode (with sun angle less than 2°) this error signal is amplified and chopped to give amplitude modulated current pulses from unidirectional power amplifiers. The pulses are sequentially routed to the drive motors of the North and South BAPTA's to give a stepped motion of the array.

The design of the OTS array system (BAPTA subsystem) is such that each of the two solar arrays may be independently rotated about the spacecraft pitch axis by

use of a ground command 'inhibit' signal. A further feature of the subsystem is that the arrays can independently offset from the satellite sun vector, either lagging or leading in incremental steps of 1.53 degrees up to maximum offsets of 21° (equinox) and 30° (solstice). Whilst the original reason for this capability was for an orbital experiment to induce 'windmill' drifts, it is also possible to use this mode of operation as a simulated error to control BAPTA orientation in the unlikely event of a catastrophic failure of the sensing circuits.

Analogue simulations of the spacecraft pitch loop and BAPTA subsystem were performed parametrically to predict BAPTA and spacecraft performance under a variety of conditions. In a friction stabilised system such as the OTS BAPTA it is essential that friction is both predictable and stable. In normal mode operation, that is when the BAPTA is sun tracking, the value of friction is relatively unimportant, but in certain back-up modes where the spacecraft is required to slew to reacquire the sun, then friction is necessary, in order to hold the array position with respect to the spacecraft body. In order to satisfy this condition the BAPTA friction F would need to be greater than the expression below assuming a rigid array on spacecraft body:

$$F = \frac{I_A \cdot T_J}{I_{S/C}}$$

where I_A = Array inertia

T_J = Couple generated by the spacecraft control thrusters

$I_{S/C}$ = Inertia of the spacecraft about the pitch axis

In practice of course the expression is more complex to take account of the array flexibility.

Array inertias of up to 100kgm² were simulated together with friction levels between 0.04 and 0.24Nm.

FLIGHT MECHANISM DESIGN

Having satisfactorily demonstrated the feasibility of the direct drive principle, it was necessary to refine and implement the essential features of the LSM into a flight solar array drive, referred to as the BAPTA (Bearing and Power Transfer Assembly). From the experience gained during the LSM programme the following main conclusions were drawn:-

- Selection of material for the bearing housing and shaft together with the preload system was critical. The design of the LSM was such that the mechanism friction torque remained insensitive to thermal gradients.

- The lead lubrication of the bearings together with the silver/copper/molybdenumdisulphide composite brushes gave excellent results.
- The use of silver sliprings was questionable due to atmospheric corrosion problems.
- Because of the low duty cycle of the operational BAPTA, a brushed motor drive can be used.

The design of the BAPTA is best examined by reference to Figure 6. The design shares many of the features of the LSM particularly with respect to points 1 and 2 mentioned above. The common features are the bearings and preload system, lead lubrication, use of an off loading mechanism, beryllium main housing and shaft and finally the cantilevered modular slipring assembly. Significant changes are the deletion of the position encoder, this function being performed by the solar array sun sensor, and the use of a brushed d.c. motor. A short discussion of the major modifications follows.

Off-Loading Mechanism

An off-loading mechanism of similar design to that of LSM has been embodied into the BAPTA. The major difference being the use of a pyrotechnic pin puller in preference to the cable cutter as the prime release mechanism. The off-loading lever is held in position by means of a calibrated spring washer reacting through the BAPTA housing via the pin puller.

The pin puller is of the dual cartridge single bridgewire type, with each cartridge having the capacity to activate the off-loading mechanism. Leakage of the gaseous pyrotechnic products is prevented by a double 'O' ring seal.

Sliprings

Two major changes to the slipring design were made:-

- Trailing and leading brushes were replaced with symmetrically seated brushes because of the desire to maintain interchangeability between north and south BAPTA's.
- A gold plated slipring replaced the silver slipring to eliminate the progressive atmospheric corrosion experienced with silver.

This latter point was of particular concern in that the OTS BAPTA is controlled by signals derived in the array mounted sun sensor and then transmitted to the control electronics by means of the BAPTA sliprings. In normal mode operation

a 7mV signal can be expected, giving rise to currents in the order of a few micro amps. Although contact resistances of tens of thousands of ohms would be needed to cause significant sun following errors it was considered desirable to avoid use of materials which could result in high impedance contact resistances. Consideration was also given to the possibility of high electrical resistance polymers being produced due to the rubbing action of the brushes and sliprings in an organic atmosphere.

In the spacecraft it can be expected that low concentrations of organic vapour, resulting from outgassing of hydrocarbon based materials, will exist, however these low concentrations together with low rubbing rates are unlikely to give rise to polymer type film. Tests are, at the time of writing, being conducted on a standard slipring system in an environment simulating the spacecraft in terms of organic vapours. The test fluid for these tests has been collected from various spacecraft thermal vacuum tests.

For the OTS BAPTA application 4 pairs of power sliprings carry up to 3 amps with a further pair of power sliprings available for other OTS derivatives. Thus for the 31 slipring combination, 12 sliprings are sized for power and 18 have been sized for signal with respect to the lead wires only. The remaining 1 ring is for earth bonding. The rings and brushes themselves have all been designed to carry current up to 6 amps giving an overall theoretical transfer capacity of 4.5k watts.

Motor Drive

A brushed d.c. Inland motor is used to drive the BAPTA with a redundant motor housed at the outboard end of the BAPTA.

The copper commutators are gold plated to prevent atmospheric corrosion and the brush material is identical to that used for the slipring brushes i.e., silver/molybdenum disulphide/copper.

MECHANISM TEST AND DEVELOPMENT

The principle objectives of the OTS BAPTA development test programme were:

- To demonstrate BAPTA performance was insensitive to the thermal environment.
- That the signal sliprings, particularly the BAPTA control slipring would not degrade due to self contamination or spacecraft contamination arising from the use of various hydrocarbon and silicon based materials.

- To demonstrate by means of accelerated life testing that BAPTA friction is predictable over a life time of 7 years.

One Engineering and four flight BAPTA's have been built. One of these BAPTA's, the Qualification Unit, was subjected to qualification level vibration and thermal vacuum testing prior to being put onto a 7 year accelerated life test. In addition to these five units a further dummy BAPTA with representative sliprings and brushes was built for special spacecraft compatibility tests, aimed at proving the integrity of the sliprings whilst working in an organic vapour atmosphere. At the time of writing these tests were not completed, but no problems relating to slipring performance had as yet been experienced.

Functional testing of the BAPTA under the ambient conditions within a clean area, were carried out using a solar array simulator whose inertia and first mode natural frequency was representative of the OTS flight array, i.e., 2.2kgm² and 1.9Hz.

During these tests a typical sensor output signal of 7mV was transferred across the sliprings and in series with a representative load impedance of 30k ohm. These tests were carried out to demonstrate that with low currents of the order of a few micro amps, the contact resistance would remain constant. No measurable change in contact resistance was noted even when control signals of 0.1mV were used in the tests. Typical average contact resistances were 5m ohm per brush.

Average motor current during these pre thermal vacuum tests was 117mA with an average Sun following error of 0.78 degrees.

Thermal vacuum tests could not be conducted easily with a representative load inertia, but offered the advantage that in the steady state case with low inertia the current taken by the motor is directly representative of BAPTA friction torque. This offered an opportunity to monitor BAPTA friction directly.

From Figure 7 (which is a graph of motor current/BAPTA friction torque against various operational environments), two points emerge which are worthy of note.

The BAPTA friction torque apparently reduces when exposed to vacuum and only after a short period of running. The reduction in friction experienced at this stage of testing is probably not due to a running in phenomenon, the number of revolutions being small compared for example to the ambient pressure functional tests.

Secondly, the BAPTA friction was apparently insensitive to the thermal environmental temperature, with the friction torque being comparable at -20°C soak to +50°C soak.

All of the 4 flight BAPTA's exhibited very similar friction characteristics during acceptance testing.

At the time of writing the life test BAPTA had completed 3 years of accelerated testing the results of which are presented in Figure 8.

From Figure 8 the average motor current during 3 years of accelerated life testing was 30.33 milliamps (0.071Nm) with a standard deviation of 2.31 milliamps (0.005Nm).

The friction level at the beginning of life testing was similar to that at the completion of the qualification programme. A rapid fall in friction resulted during the first few days of the 1 rev per hour test, after which the friction level apparently remained fairly constant. No significant trend in friction could be identified as a result of wear or long term vacuum exposure or due to changes in the environmental boundary temperatures.

FUTURE DEVELOPMENTS

The OTS BAPTA is at present being examined to identify the growth potential for power transfer and load carrying capacity. To date these investigations have shown that power transfer capability of up to 4.5kW is feasible but requires some minor modifications to the slipping wire gauges and the BAPTA thermal model.

Thus all combinations of signal rings and power rings up to a total of 31 rings are possible with minimum modifications. Because the slipping assembly is of modular design, being cantilevered off the shaft, it is also possible to extend the length of the slipping assembly and embody additional rings possibly up to 40 in total.

In the OTS BAPTA configuration 7 of the 18 signal rings are used for control of the BAPTA Sun pointing vector. In order to allow greater flexibility to the Power subsystem designer, it is proposed in future to use a 1200 step stepper motor thus vacating 7 additional rings for use as power or signal transfer.

A stepper motor driven BAPTA is expected to undergo test in August, 1977.

Table 1
LSM Design Requirements

Operating Speed	Normal 4 rev/day, Acquisition 1 deg/sec.	
Life	In orbit 7 years, Ground Running 50 hours	
Slipring	6 Channels (Double Circuit) 2.5A Nominal 5A Peak 1 Bonding Channel 12 Channels 0.05A.	
Qualification Environment		
Static Load	A single load of 1750N at the drive flange. Applied for 5 mins. along six directions corresponding to an orthogonal axes set containing the rotational axis.	
Constant Acceleration	18g applied for 5 mins. Axes as above.	
Sinusoidal Vibration	Axes as above. Sweep rate 2 octaves/min. 5 to 15Hz.; 9mm zero to peak displacement. 15 to 200Hz.; 8g zero to peak acceleration.	
Random Vibration	Axes as above. Duration 5 mins. each axis. 25 to 100Hz.; 3dB/Oct. increasing to 0.2g²/Hz. 100 to 2000 Hz.; 0.2g²/Hz. flat.	
Thermal Vacuum	T₁ = Shaft temperature at drive flange °C.	
	T₂ = Shroud or radiator sink temperature °C.	
Duration Hours	T₁	T₂
8	20	-25
8	80	15
8	80	80
8*	70	45
*During this period, four 72 minute eclipses are required to be submitted by decreasing T₁ to -30°C whilst maintaining T₂ at 45°C.		

Table 2
LSM Life Test Schedules

T₁ = Temperature of Drive Flange

T₂ = Enclosing shroud or sink temperature

(A) Accelerated Test

Total test duration 15 cycles each comprising:-

8 Eclipse simulations with T₂ = 22.5°C, T₁ varying from 60 to -20°C in 72 minutes. Speed 1 rev/day. Each Eclipse followed by an acquisition of 1 revolution at 1°/sec.

10 Days at 1 rev/hour with T₂ = 22.5°C, T₁ = 60°C for odd number cycles.

10 Days at 1 rev/hour with T₂ = 22.5°C, T₁ = 10°C for even number cycles.

Total number of revolutions including qualification testing = 3911.

(B) Real Time Life Test

Speed - 1 rev/day.

Cycle period is 26 weeks each cycle comprising:-

6 weeks (or 5 days) with 1 Eclipse simulation per day having T₁ varying from 60 to -20°C in 72 minutes and T₂ = 22.5°C. Mechanism then completes 1 revolution.

20 weeks with T₂ = 22.5, T₁ = 60°C for odd number cycles.

20 weeks with T₂ = 22.5, T₁ = 10°C for even number cycles.

Number of cycles completed 5 (2½ years).

Table 3

LSM Real Time Test Data (Averaged Values)

Cycle	Week	T ₁ (°C)	Pressure (Torr)	Error (Degrees of Arc)	Torque Nm	MP (Watts)
1	1	60	1 x 10 ⁻⁶	-3.7	0.104	1.3
	13	60	3 x 10 ⁻⁷	-3.0	0.084	1.1
	26	60	1.8 x 10 ⁻⁷	-3.0	0.084	1.1
2	1	60	1.6 x 10 ⁻⁷	-3.0	0.084	1.2
	13	10	3.5 x 10 ⁻⁸	-2.5	0.070	1.0
	26	10	3.0 x 10 ⁻⁸	-2.4	0.067	1.0
3	1	60	1.8 x 10 ⁻⁷	-2.8	0.078	1.0
	13	60	1.5 x 10 ⁻⁷	-2.4	0.067	0.8
	20	60	1.0 x 10 ⁻⁷	-2.9	0.081	0.7
	26	60	8.1 x 10 ⁻⁸	-2.4	0.067	0.8
4	1	60	8.2 x 10 ⁻⁸	-2.4	0.067	0.8
	7	10	2.2 x 10 ⁻⁸	-2.5	0.070	0.8
	13	10	1.7 x 10 ⁻⁸	-2.25	0.063	0.6
	20	10	1.5 x 10 ⁻⁸	-1.9	0.053	0.6
	24	10	1.7 x 10 ⁻⁸	-2.1	0.058	0.6
5	1	60	6.6 x 10 ⁻⁸	-2.6	0.073	0.7
	7	28*	3.3 x 10 ⁻⁸	-2.4	0.067	0.7
	12	28*	2.7 x 10 ⁻⁸	-2.4	0.067	0.7
	15	28*	3.5 x 10 ⁻⁸	-2.4	0.067	0.75
	16	60	3.5 x 10 ⁻⁸	-2.4	0.067	0.75

* Due to heater failure.

Table 4
Key Features of BAPTA Subsystem

- Totally redundant sensing and drive channels (i.e. Sun sensors, electronics and motor).
- Control signals derived from solar array mounted Sun sensors.
- Normal mode Sun tracking error less than 2° . Initiation of normal mode is by ground command only. Loss of Sun presence in either acquisition or normal mode causes arrays to stop until the next ground command.
- Automatic failure detection which disconnects BAPTA control electronics from the AOCS.
- Independent variable offset facility of 1.53° slip up to a maximum offset of 30° .
- Independent inhibit modes.
- Nominal slew rate of 1° second.
- Saturated torque demand at 2° .
- Sequential North/South actuation to minimise spacecraft pitch disturbances.
- Open loop slew mode of operation operated by ground command.
- Catch up time after exit from 18 degree eclipse will be a maximum of 15 minutes.

Table 5. Summary of BAPTA Key Features

• Mass	-	4.2kg including pyrotechnics, redundant motors and all connectors.
• Motor	-	2 brushed d.c. motors (1 being redundant) torque 0.71Nm (stall) current 0.3A at stall voltage 50 volts
• Speed	-	1 rev/day, normal mode 1° /sec Sun acquisition
• Power Consumption	-	Normal mode - 0.04W Acquisition - 0.85W
• Nominal Friction	-	0.07Nm (vacuum)
• Slip Rings	-	12 power rings 3 amp. 18 signal rings 1 earth bonding
• Growth Potential	-	30 power rings 6 amps. 1 earth bonding
• Launch Loads	-	1200N (OTS)
• Array Latch Loads	-	100Nm
• Stiffness, Caged	-	Axial 100×10^6 Nm Radial 40×10^6 Nm/rad.
Operational	-	Axial 1×10^5 Nm Radial 20×10^3 Nm/rad.
• Temperature Limits	-	-45 to $+55^\circ$ C Shaft 0 to $+55^\circ$ C Housing
• Environmental Test	-	Acceleration $\pm 18g$ Vibration along 3 principal axes Sine 15 to 21Hz 7.5g 21 to 100Hz 2.5g Random 20 to 60Hz $0.06g^2/Hz$ 60 to 300Hz 3dB/octave to $0.25g^2/Hz$ 300 to 1200Hz $0.25g^2/Hz$ 1200 to 2000Hz decrease at 6dB/octave

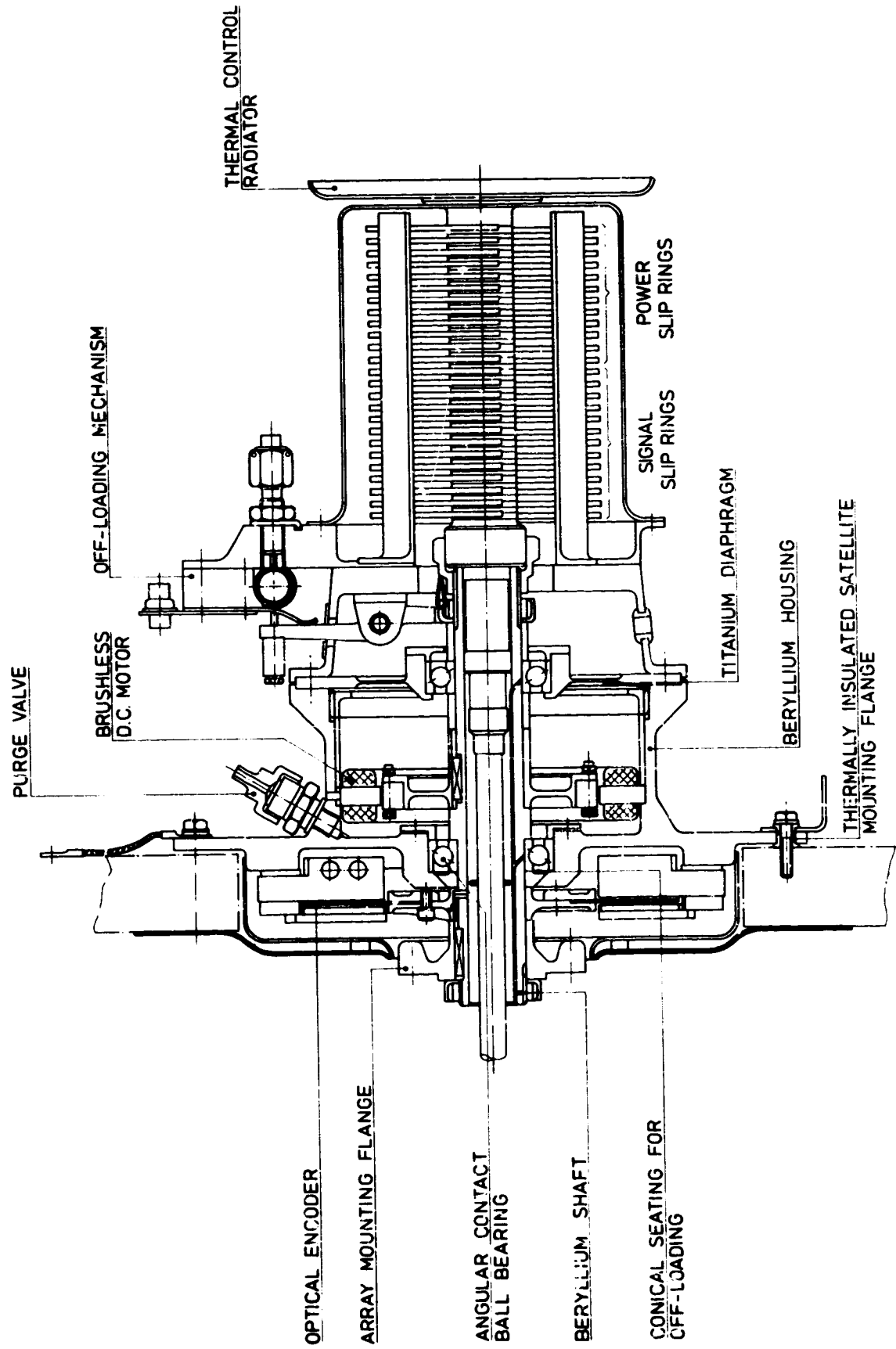


Figure 1. Overall Assembly of Low Speed Mechanism

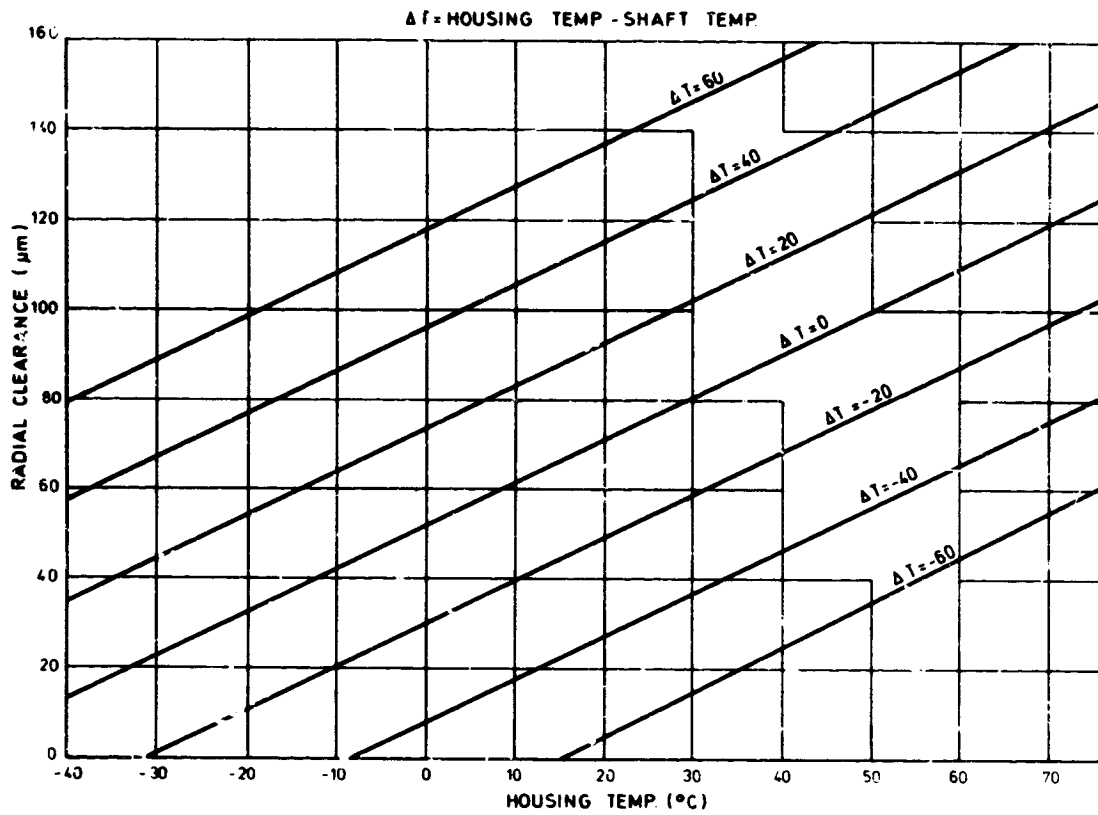


Figure 2. Bearing Radial Clearance Vs Temperature (Al/Al)

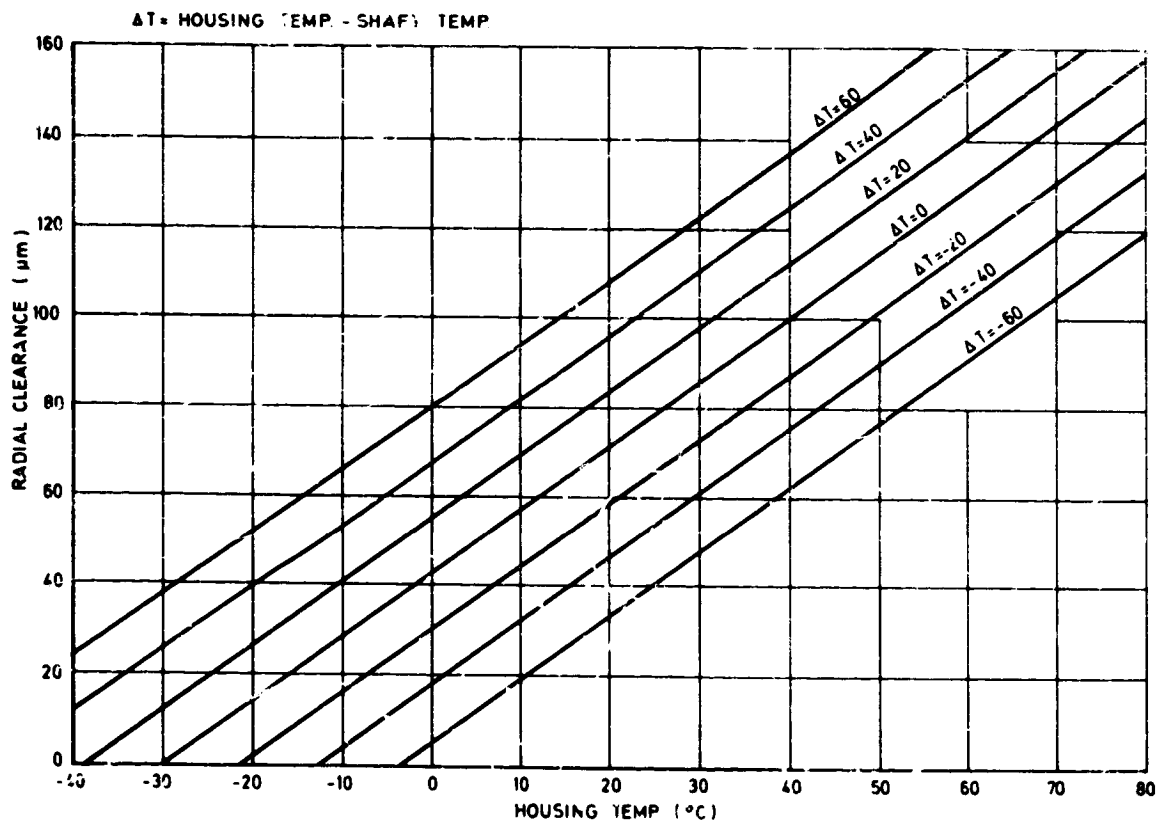


Figure 3. Bearing Radial Clearance Vs Temperature (Be/Be)

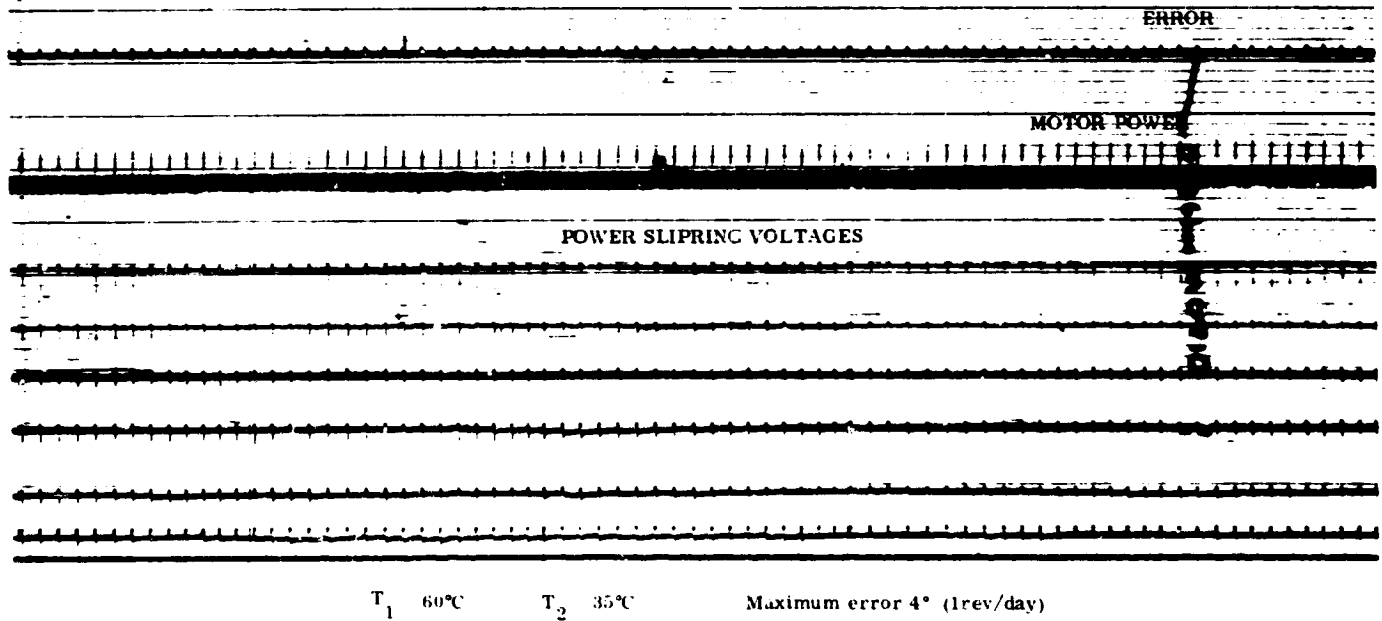


Figure 4. LSM Following Error During Eclipse Simulation

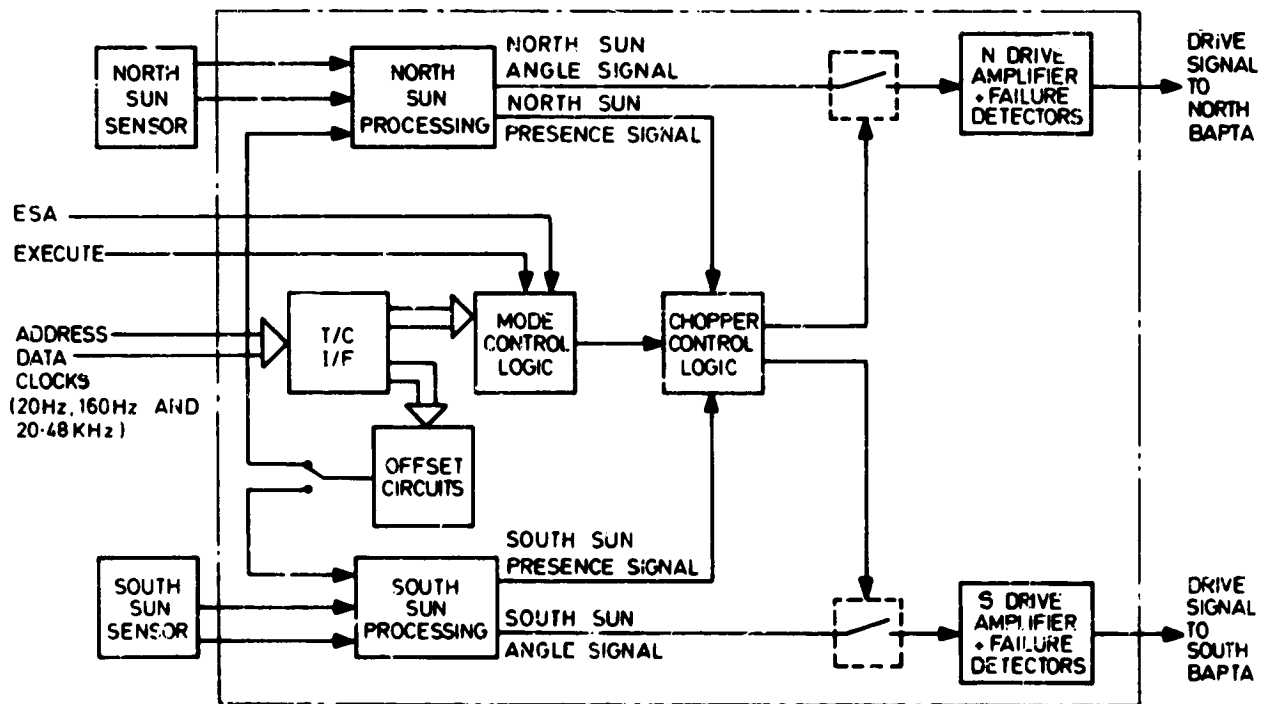


Figure 5. System Block Diagram

REPRODUCIBILITY OF THE
PAGE IS POOR

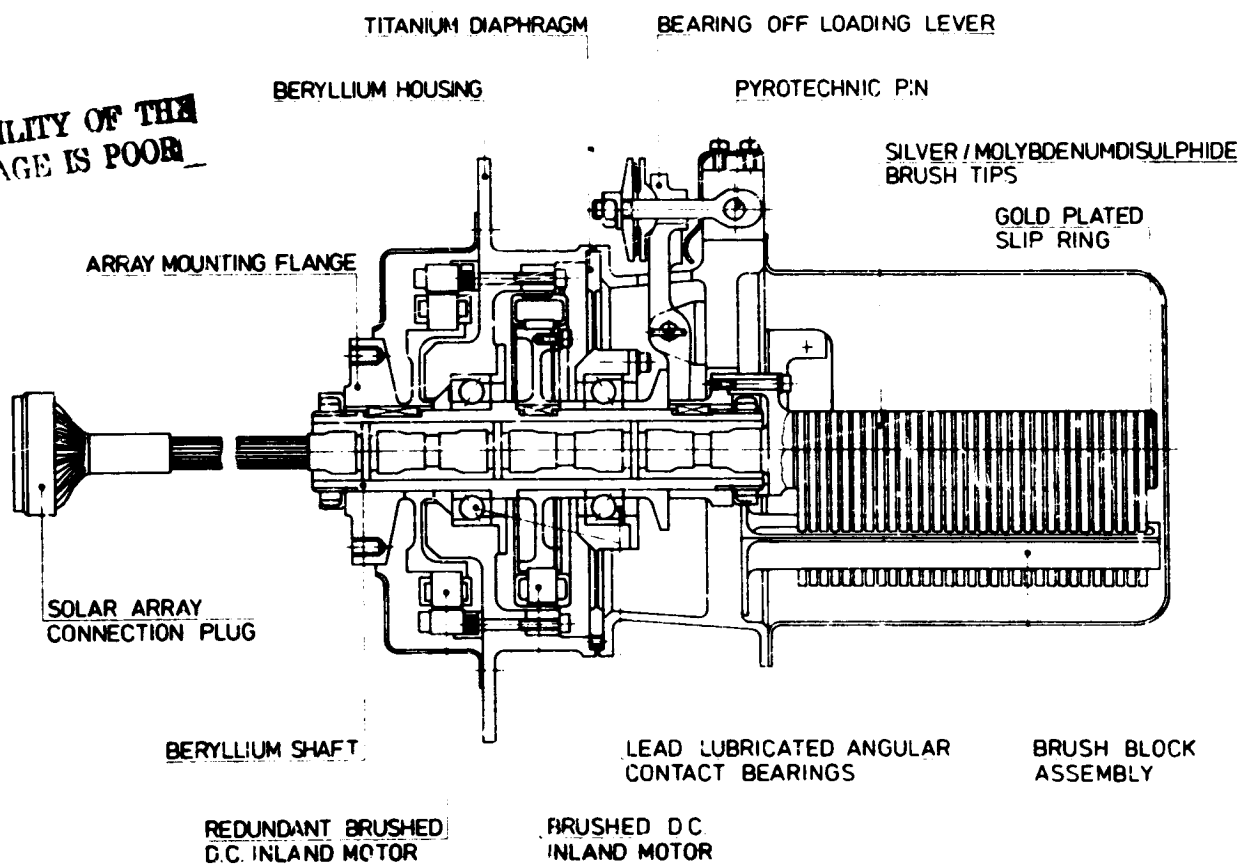


Figure 6. OTS BAPTA General Assembly

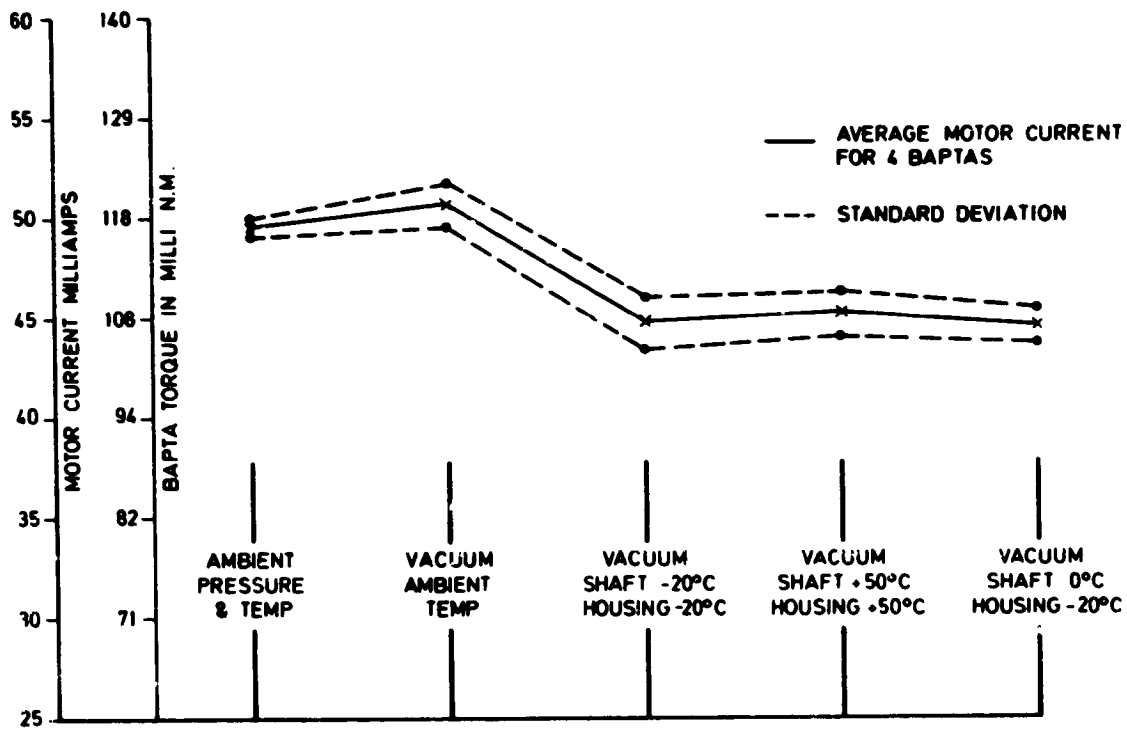


Figure 7. BAPTA Friction for Various Operational Environments

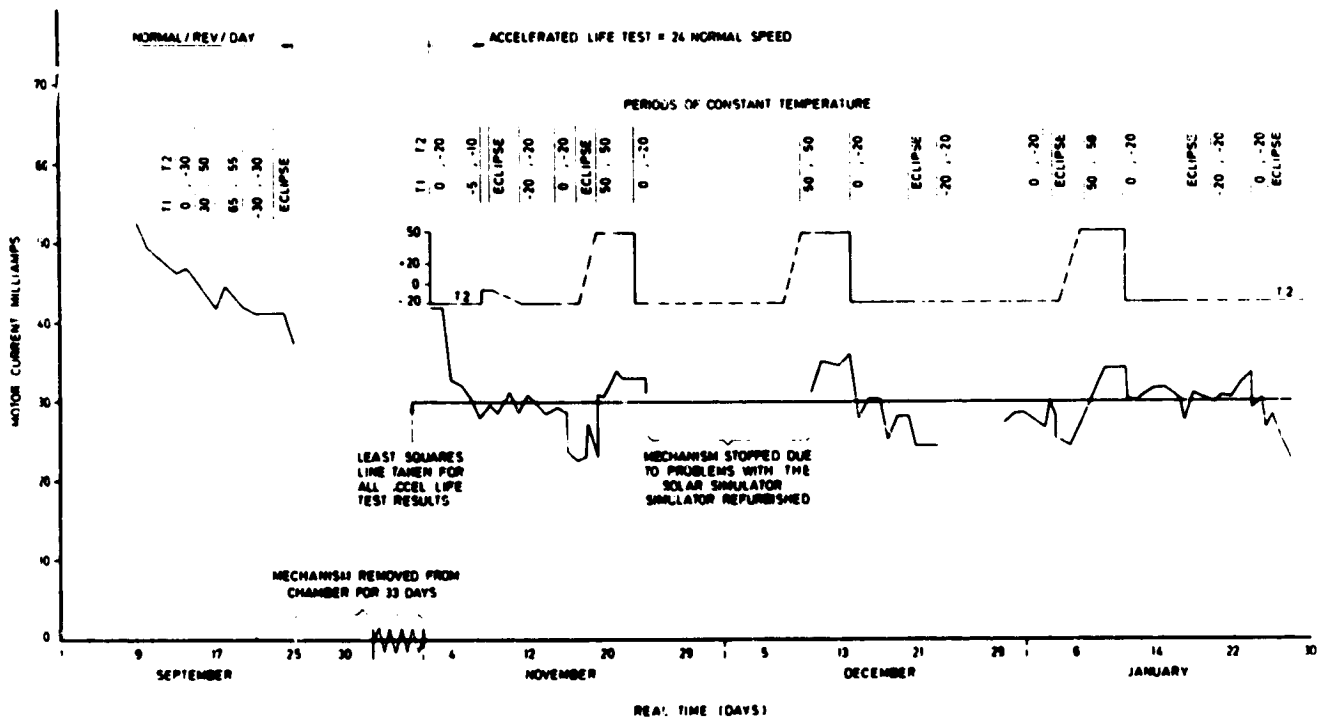


Figure 8. BAPTA Life Test Results

VIKING MECHANISMS: A POST MISSION REVIEW

Vernon P. Gillespie
NASA, Langley Research Center

During the summer of 1976 the United States successfully landed two Viking Spacecraft on the surface of Mars. This feat and the subsequent scientific exploration was made possible by the successful operation of numerous aerospace mechanisms on both the landers and the orbiters. The goal of the NASA Viking program is to learn more about the planet Mars with the primary emphasis on biological, chemical, and environmental aspects which are relevant to the existence of life.

This presentation will review the current scientific results of the Viking mechanisms. Special attention will be given to the four known mechanism anomalies. Reflecting on the success of the Viking spacecraft, the author will discuss recommendations for the design of future aerospace mechanisms.

**END
DATE
FILMED**

APR 21 1978